IMPLICIT UPWIND METHODS FOR THE EULER EQUATIONS

83-1930

A83-39382

W.A. Mulder*
University Observatory
Leiden, the Netherlands.

B. van Leer**
University of Technology
Department of Mathematics and Computer Science
Delft, the Netherlands

Abstract

Implicit difference schemes for the one-dimensional Euler equations with conservative upwind spatial differencing and linearization in time are tested on a problem of steady discontinuous flow. Fastest convergence (quadratic for the first-order "backward Euler" scheme) is obtained with upwind switching provided by Van Leer's differentiable split fluxes, which easily linearize in time. With Roe's non-differentiable split flux-differences the iterations may get trapped in a limit cycle. This also happens in a second-order scheme with split fluxes, if the matrix coefficients arising in the time-linearization are not properly centered in space. The use of split second-order terms computed from split fluxes degrades the accuracy of the solution, especially if these are subjected to a limiter for the sake of monotonicity preservation. Second-order terms computed from Riemann invariants perform best.

1. Introduction

Implicit time-dependent methods for computing steady inviscid flows have been around from some time[1], but there have been few applications with strong shocks. In particular, the influence of a shock wave on the convergence to a steady state is not well known. The aim of this paper is to study in detail the performance of one implicit method for time-integration of the one-dimensional Euler equations using conservative upwind-biased spatial differencing for a proper treatment of shocks.

The implicit method, "backward Euler", is formulated in Sec. 2. It is tested on a one-dimensional model of the isothermal flow in a spiral galaxy, described in Sec. 3. Computations of this flow with explicit methods were made by Van Albada et al.[2]. It makes a good test problem, because of the strong shock (Mach 2.5) and the cyclic space coordinate that prevents disturbances to leave the computational domain.

The performance of schemes with first-order spatial accuracy is described in Sec. 4. First, Roe's[3] approximate solution of the Riemann problem for neighboring cells is used to provide the upwind switching, with a modification to exclude expansion shocks. Then we use flux-vector splitting[11], with continuously differentiable flux-vectors according to Van Leer[4].

The latter method is also used in the schemes with second-order spatial accuracy tested in Sec. 5. Such accuracy can be achieved by assuming a set of independent state quantities to have linear distributions in each cell, rather than uniform distributions, as with first-order schemes. The slope of a linear distribution can be found through a difference-averaging procedure constrained by the monotonicity condition[5]. The averaging was applied to differences of various sets of quantities: the split flux-vectors, variables related to the Riemann-invariants, and the correct Riemann invariants.

Section 6 contains the main conclusions of the paper.

2. Formulation of the method

Let w denote the vector of M conserved state quantities, f(w) the corresponding flux-vector and s(w,x) the source-term vector. The space co-ordinate is x, time is t. We wish to find a stationary solution for w of the partial differential equations:

$$\frac{\partial w}{\partial t} = - \frac{\partial f}{\partial x} + s \equiv g \; , \tag{1}$$

which is equivalent to the problem of determining w such that g vanishes.

In order to discretize Eq. (1) we define a grid with N zones centered at the points x_i, separated by Δx. Time at iteration step n is denoted by t^n, the timestep by Δt^n, so $t^{n+1} = t^n + \Delta t^n$. Differences with respect to time are written as $\Delta_t w = w^{n+1} - w^n$ and with respect to space as $\Delta_{i+\frac{1}{2}} w = w_{i+1} - w_i$. Here w_i represents the zone-averaged value of w.

Let W be the vector consisting of NxM elements w_{ki} (k=1,2,...,M and i=1,2,...,N), and let G be defined analogously with elements g_{ki}. The implicit scheme can be written in "delta form"[1] as

$$L^n \Delta_t W \equiv \left[\frac{1}{\Delta t^n} - \alpha\left(\frac{\partial G}{\partial W}\right)^n\right] \Delta_t W = G^n \; , \tag{2}$$

where $\frac{\partial G}{\partial W}$ is the Jacobian of G with respect to W. For $\alpha=0$, Eq. (2) reduces to an explicit scheme, for $\alpha=1$ (backward Euler or implicit Euler scheme) and $\Delta t^n \to \infty$ we have Newton's method for finding a root, with quadratic convergence.

The right-hand-side G^n of Eq. (2) contains all the physics of the problem and defines the accuracy of the solution. The matrix L^n controls the convergence process.

Newton's method will work properly if W is sufficiently close to the stationary solution. Therefore, the scheme is started with a small Δt^n to let the iteration process mimic an explicit, time-accurate integration. Once W starts feeling the attraction of the final solution, Δt^n may become large and, if $\alpha = 1$, Newton's method starts working.

---
*Research Assistant
**Research Scientist. Member AIAA.

The stage of convergence can be monitored by

$$\mathrm{RES}^n = \max_{k,i} \frac{|g_{ki}^n|}{|w_{ki}^n| + h_{ki}^n}, \quad k=1,2,\ldots,M, \; i=1,2,\ldots,N, \quad (3)$$

where h_{ki} is some positive constant that prevents division by zero. The time-step is derived from this quantity according to:

$$\Delta t^n = \varepsilon/\mathrm{RES}^n. \quad (4)$$

Eq. (4) guarantees that in the <u>explicit</u> case (α=0) the relative change of the state quantities per time-step will nowhere exceed ε :

$$\frac{|\Delta_t w_{ki}|}{|w_{ki}^n| + h_{ki}^n} < \varepsilon \quad k=1,2,\ldots,M \text{ and } i=1,2,\ldots,N.$$

3. The test problem

The test problem, due to Woodward[12] and used previously for a comparison[2] of explicit methods, is briefly summarized below. It describes the flow of isothermal gas along an almost circular path through the stellar gravitational field of a rotating two-armed spiral galaxy. The vector of conserved quantities in this case is:

$$w = \begin{pmatrix} \rho \\ \rho u \\ \rho v \end{pmatrix}, \quad (5a)$$

where ρ is the density, u the velocity perpendicular to and v the velocity along the spiral arms. The space-coordinate x measures distance perpendicular to the arms; vector of fluxes in this direction is:

$$f = \begin{pmatrix} \rho u \\ \rho(u^2 + c^2) \\ \rho uv \end{pmatrix}, \quad (5b)$$

with c the effective sound speed, a constant. The source-term vector is:

$$s = \begin{pmatrix} 0 \\ 2\Omega\,(v-v_o)\rho + \frac{2}{\alpha r}\rho A \sin\eta \\ -\frac{\kappa^2}{2\Omega}(u-u_o)\,\rho \end{pmatrix}. \quad (5c)$$

Here $\Omega = \Omega(r)$ is the angular velocity at a radius r with respect to the centre of the galaxy. The spiral arms are assumed to be tightly wound, with small pitch angle θ_s. The unperturbed velocities are approximately $v_o = r(\Omega - \Omega_p)$ and $u_o = \alpha r(\Omega - \Omega_p)$, where Ω_p is the pattern speed of the rapidly rotating spiral pattern and $\alpha = \sin\theta_s << 1$. The epicycle frequency κ is given by $\kappa^2 = \frac{2\Omega}{r}\frac{d}{dr}(r^2\Omega)$, A is the amplitude of the spiral perturbation on the gravitational field, and η is the spiral phase defined by $\eta = \frac{2x}{\alpha r}$. The source term with A is due to the gravitational field, the other source terms are due to the Coriolis force. The problem is periodic: $w(\eta+2\pi,t) = w(\eta,t)$. A procedure to find the stationary solution by integrating the stationary differential equations is given by Roberts[6]. For sufficiently large A this solution is transonic and discontinuous.

The parameters are chosen as is thought to be appropriate for the solar neighbourhood: Ω = 25 km s^{-1} kpc^{-1}, κ = 31.3 km s^{-1} kpc^{-1}, Ω_p = 13.5 km s^{-1} kpc^{-1}, c = 8.56 km s^{-1}, r = 10 kpc, $\alpha = \sin(6°.7)$ and A = 72.92 (km s^{-1})^2.

All calculations started from uniform initial values:

$$\rho_i^o=1, \; u_i^o=u_o, \; v_i^o=v_o, \; i=1,2,\ldots,N. \quad (6)$$

The constants h_{ki} in Eq. (3) are chosen to be:

$$h_{1i} = 0, \; h_{2i} = \rho_i c, \; h_{3i} = \rho_i c, \; i=1,2,\ldots,N. \quad (7)$$

Finally, we mention that the source-terms are linear in w:

$$s = Bw, \quad (8a)$$

$$B(x) = \begin{pmatrix} 0 & 0 & 0 \\ -2\Omega v_o + \frac{2A}{\alpha r}\sin\eta & 0 & 2\Omega \\ \frac{\kappa^2 u_o}{2\Omega} & \frac{-\kappa^2}{2\Omega} & 0 \end{pmatrix}. \quad (8b)$$

4. First-order accurate results.

Up to this point we have discretized Eq. (1) in time, yielding Eq. (2), and we have specified the source term. We now have to discretize in space in order to evaluate $\frac{\partial f}{\partial x}$. This is done by upwind differencing in two different ways: (i) using Roe's[3] linearized Riemann solution and (ii) using Van Leer's[4] flux-vector splitting. For a comprehensive review of upwind-differencing techniques the reader is referred to Harten, Lax and Van Leer[7].

4.1 Roe's approximate Riemann solver

An upwind method of discretizing the flux derivative $\frac{\partial f}{\partial x}$ has been described by Roe[3,8]. We included Roe's own modification to suppress expansion shocks, reported elsewhere[9]. The right-hand-side of Eq. (2) becomes:

$$g_i^n(w_{i-1}, w_i, w_{i+1}) = B_i w_i - \frac{1}{\Delta x}(A^+_{i-\frac12}\Delta_{i-\frac12}w + A^-_{i+\frac12}\Delta_{i+\frac12}w),$$
$$i=1,2,\ldots N, \quad (9)$$

where A^+ and A^- are the positive and negative part of $A \equiv \partial f/\partial w$ and depend on w. Roe's approximate Riemann solver includes a simple recipe to calculate these matrices but their derivatives, needed on the left-hand-side of (2), are costly to compute and do not even exist in shocks and around sonic points. We therefore freeze $A^{\pm}$ at the old level when deriving $\frac{\partial g}{\partial w}$. Eq. (2) becomes:

$$[-\frac{\alpha}{\Delta x}A^+_{i-\frac12}]\,\Delta_t w_{i-1}$$
$$+[\frac{1}{\Delta t^n} - \alpha B_i + \frac{\alpha}{\Delta x}A^+_{i-\frac12} - \frac{\alpha}{\Delta x}A^-_{i+\frac12}]\,\Delta_t w_i$$
$$+ \; [\frac{\alpha}{\Delta x}A^-_{i+\frac12}]\,\Delta_t w_{i+1} = g_i^n, \; i=1,2,\ldots,N, \quad (10)$$

giving the matrix L^n a cyclic block-tridiagonal structure. At this point we remark that if a matrix M_i^n is defined by:

$$M_i^n = B_i - \frac{1}{\Delta x}(A^+_{i-\frac12}\Delta_{i-\frac12} + A^-_{i+\frac12}\Delta_{i+\frac12}), \quad (11)$$

then Eq. (10) can be rewritten as:

$$[\frac{1}{\Delta t^n} - \alpha M_i^n]\,\Delta_t w = M_i^n w_i^n,\quad i=1,2,\ldots,N. \qquad (12)$$

The matrix on the left-hand-side of this equation differs from the one in Eq. (2), but this does not matter if $g_i^n = M_i^n w_i^n$ ultimately vanishes.

The convergence behavior of this scheme is given in Figure 1a, for α=1, N=64 and ε=0.5. Plotted is ${}^{10}\log\,(\mathrm{RES}^n)$ as defined in Eqs. (3) and (7) versus the number of iteration steps n. After some almost explicit searching the convergence process sets in, but it suddenly stops. Closer inspection reveals that the solution jumps symmetrically up and down across the correct solution: the convergence process is locked in a two-vector limit cycle. An analysis of Eq. (12) makes this comprehensible. For α=1 and large Δt^n we have:

$$-M^n \,\Delta_t w = M^n w^n\ , \qquad (13)$$

implying that $M^n w^{n+1} = 0$, but not necessarily $M^{n+1} w^{n+1} = 0$ which is actually desired. For the two solutions in the limit cycle we find the following, almost exact, relation:

$$M^{n+1} w^{n+1} = -\,M^n w^n. \qquad (14)$$

Neglecting terms of the order $O((\Delta_t w)^2)$ we can write the left hand side as:

$$M^{n+1} w^{n+1} = M^{n+1} w^n + M^{n+1}\,\Delta_t w = M^{n+1} w^n + M^n\,\Delta_t w$$

$$= M^{n+1} w^n - M^n w^n = (\Delta_t M)\; w^n. \qquad (15)$$

Thus we are confronted with the fact that the time derivative of $A^{\pm}$, hence of M, was neglected earlier.

It is worth mentioning that a run with fixed boundary values, taken from the exact solution, converged properly (Fig. 1b). Clearly the boundaries provide enough damping to avoid the limit cycle.

Being aware of Eq. (14), we experimented with two different amendments. The most obvious remedy is to make $\alpha > 1$, implying under-relaxation. It turned out that for $\alpha \gtrsim 1.2$ the scheme converged: the convergence slowed down with increasing α. The behavior for α=1.2 is shown in Fig. 1c.

Another way out is to repair the inconsistency of Eq. (14). A consistent formulation would be $-M^{n+1}\,\Delta_t w = M^{n+1} w^n$, ensuring that $M^{n+1} w^{n+1} = 0$. On the left-hand-side we may replace M^{n+1} by M^n without reproof. In order to estimate M^{n+1} for the right-hand-side we devised a predictor-corrector method that will be referred to as the "β-scheme":

$$\text{Step 1:}\ [\frac{1}{\Delta t^n} - \alpha M^n]\,\Delta_t \tilde{w} = M^n w^n, \qquad (16a)$$

from which follow $\tilde{w}^{n+1} = w^n + \Delta_t \tilde{w}$ and $\tilde{M}^{n+1}$;

$$\text{Step 2:}\ [\frac{1}{\Delta t^n} - \alpha M^n]\,\Delta_t w = [(1-\beta)M^n + \beta \tilde{M}^{n+1}]\, w^n, \qquad (16b)$$

after which follows the final update $w^{n+1} = w^n + \Delta_t w$. For β=0 we have the old version of Eq. (11). The obvious choice β=1, does not lead to convergence. Eq. (14) suggests that $\beta=\frac{1}{2}$ at least will destroy the limit cycle. It actually does, as can be seen in Fig. 1d, with α=1.

Note that the inversion of the cyclic block-tridiagonal matrix in Step 2 is identical to the one in Step 1. Since this inversion is the most elaborate part of the scheme, the second step adds a relatively small amount of extra computer time. All together the β-scheme is almost twice as efficient as the original scheme with α=1.2.

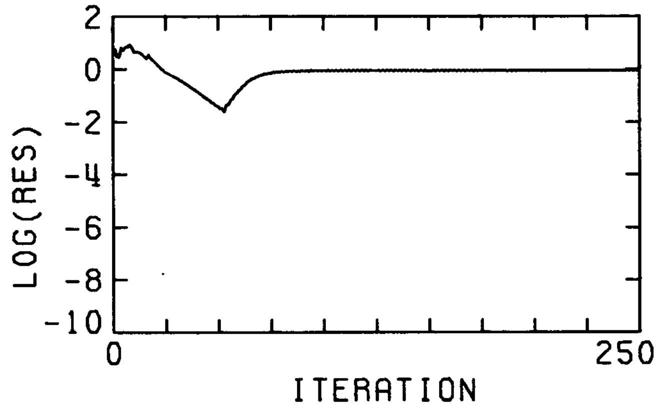

Fig. 1a. Convergence history for scheme (10), based on Roe's approximate Riemann solver. The iteration process ends up in a two vector limit cycle. Parameters: α = 1, ε = 0.5.

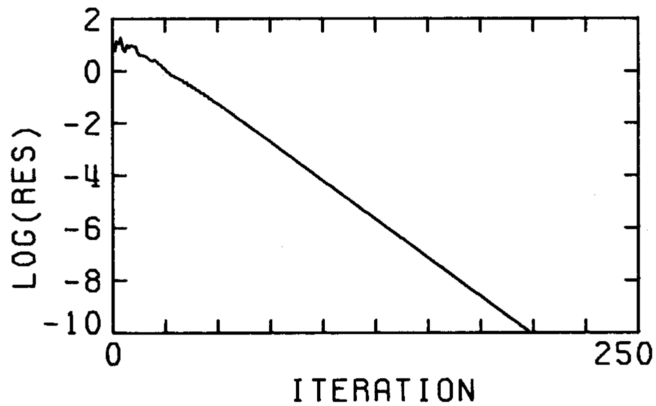

Fig. 1b. As 1a, but with fixed boundary values.

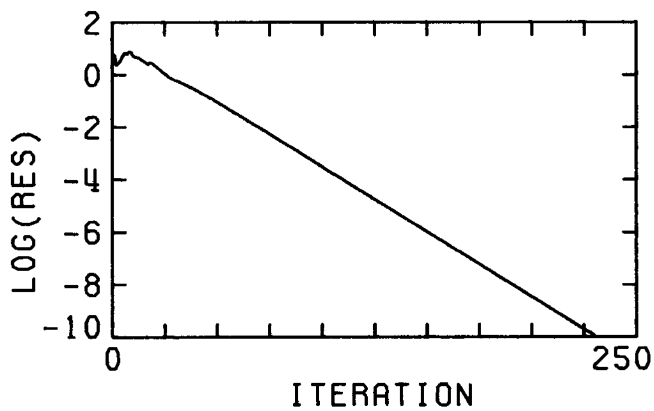

Fig. 1c. As 1a, but with α = 1.2.

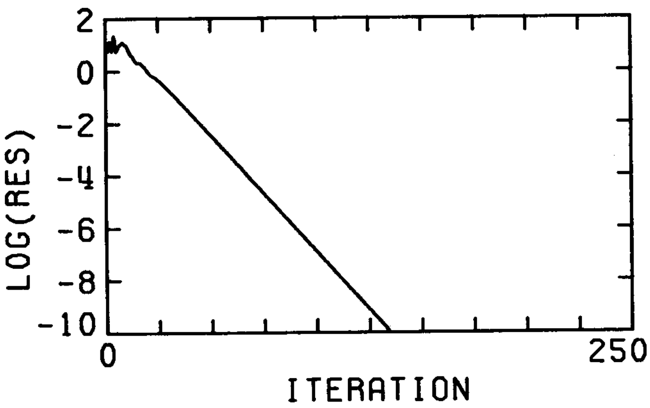

Fig. 1d. Convergence history for the β-scheme as given in Eq. (15).
Parameters: $\alpha = 1$, $\varepsilon = 0.5$ and $\beta = 0.5$.

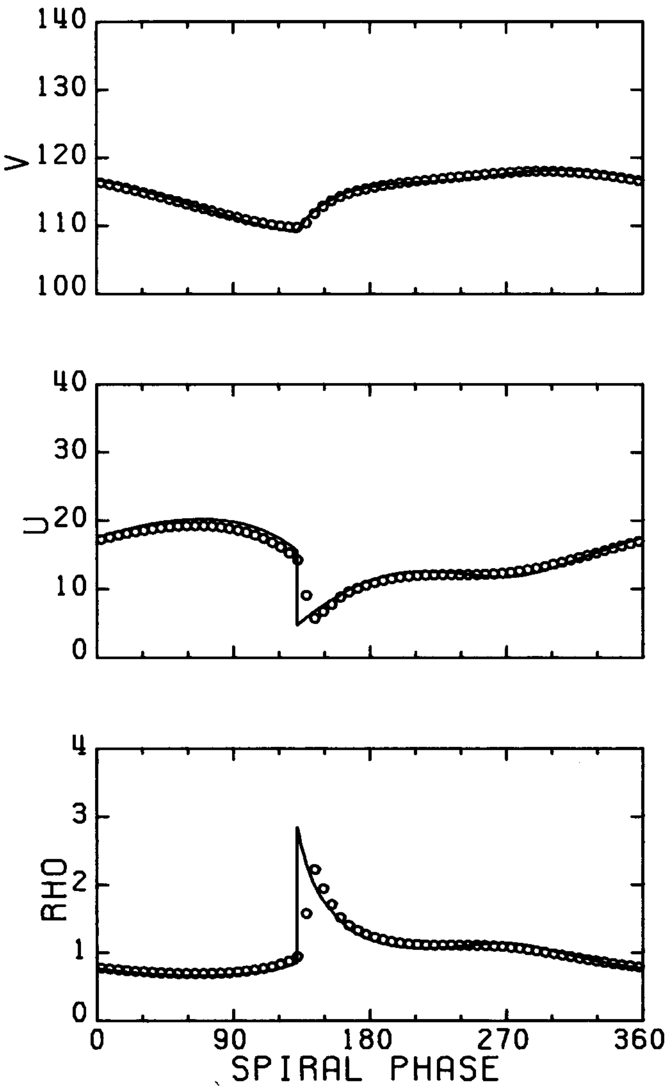

Fig. 2. The converged solution using Roe's approximate Riemann solver.

Attempts to optimize the β-scheme by choosing a linear combination of $\Delta_t w(\beta{=}0)$ and $\Delta_t w(\beta{=}\frac{1}{2})$ resulted in a somewhat faster convergence, but no significant decrease in computer time resulted because of the extra work involved.

We end this section with fig. 2, showing the converged solution of Roe's scheme.

4.2. Flux-vector splitting

In order to formulate a scheme fully consistent with Eq. (2) we need a Riemann solver that allows continuous differentiation. The simplest one is given by Van Leer [4] on the basis of flux-vector splitting, a technique due to Steger and Warming [11]. Another possibility is Osher's [10] solver, which leads to more complicated formulas and will not be considered here.

In flux-vector splitting, the flux f is considered the sum of a forward flux f^+ and a backward flux f^-. Here we use

$$f^+ = \begin{cases} f & , u > c \\ \begin{pmatrix} \frac{\rho}{4c}(u+c)^2 \\ \frac{\rho}{2}(u+c)^2 \\ \frac{\rho}{4c}(u+c)^2\, v \end{pmatrix} & , |u| < c \\ 0 & , u < -c \end{cases} \tag{17a}$$

$$f^- = f - f^+ \tag{17b}$$

We now can readily derive the Jacobian matrices $E^\pm = \frac{\partial f^\pm}{\partial w}$, needed in the implicit upwind differencing scheme.
Eq. (2) becomes:

$$\left[-\frac{\alpha}{\Delta x} E^+_{i-1}\right] \Delta_t w_{i-1}$$

$$+ \left[\frac{1}{\Delta t} - \alpha B_i + \frac{\alpha}{\Delta x} E^+_i - \frac{\alpha}{\Delta x} E^-_i\right] \Delta_t w_i$$

$$+ \left[\frac{\alpha}{\Delta x} E^-_{i+1}\right] \Delta_t w_{i+1}$$

$$= B w_i - \frac{1}{\Delta x}\left(f_i^{+} - f_{i-1}^{+} + f_{i+1}^{-} - f_i^{-}\right),$$

$$i = 1,2,\ldots,N \quad . \tag{18}$$

The matrix L again has a cyclic block-tridiagonal structure.

The improvement in convergence speed with regard to the previously described schemes is dramatic. Fig. 3a shows the convergence history: machine zero is reached in 16 steps with quadratic convergence. The solution is displayed in Fig. 3b. Comparison with Fig. 2 shows that Roe's modified scheme is superior in describing the flow near the sonic print.

We end this section with the conclusion that quadratic convergence can be achieved for discontinuous flows using an implicit first-order upwind-difference scheme with a continuously differentiable numerical flux function. We shall use the same numerical flux function in the second-order schemes of the next section.

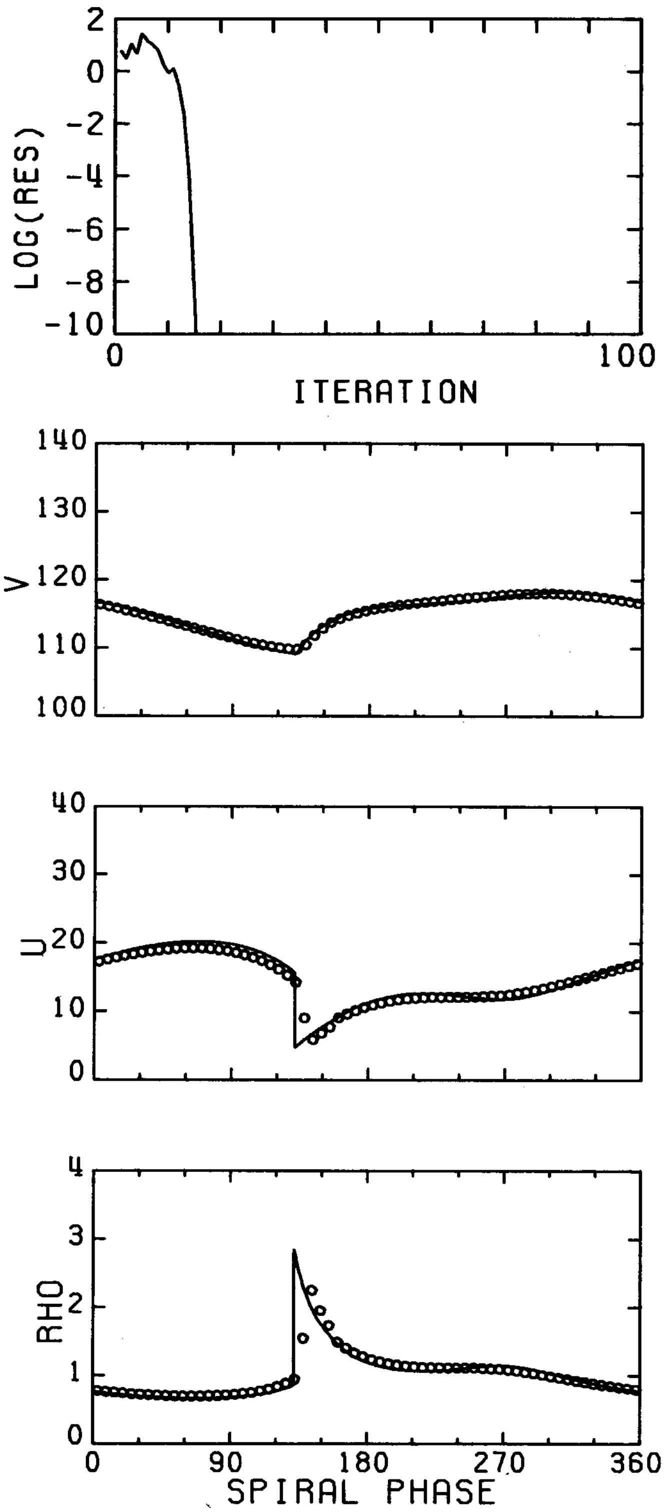

Fig. 3a. Convergence history and 3b first order accurate solution for scheme (18), using flux vector splitting.
Parameters: $\alpha = 1$, $\varepsilon = 0.5$.

5. Second-order spatial accuracy

We can achieve second-order accuracy by assuming a set of (not necessarily conserved) quantities q to have a piecewise linear distribution in each computational cell:

$$q^n(\xi) = q_i^n + \xi\,\overline{\Delta_i q^n}\,, \quad \xi \equiv \frac{x-x_i}{\Delta x}, \quad |\xi| < \tfrac{1}{2}. \qquad (19)$$

The undivided gradient $\overline{\Delta_i q^n}$, or simply $\overline{\Delta}$, is found by averaging the differences $\Delta_{i+\frac{1}{2}}\, q^n$ and $\Delta_{i-\frac{1}{2}} q^n$, or Δ_+ and Δ_-. In this way information of 3 zones is used, leading to the desired increase in accuracy. In regions where q varies smoothly an obvious way of averaging is:
$\overline{\Delta} = \delta \equiv \frac{1}{2}(\Delta_+ + \Delta_-)$. However, this is not justified at the head or foot of a discontinuity; some modification is recommended then to limit $\overline{\Delta}$ to $O(\Delta x)$. A clear account on this subject is given by Van Leer [5] on the basis of the monotonicity condition. A smooth approximation of the switches given in 5, Eq. (66) has been proposed by Van Albada [2]:

$$\overline{\Delta} = \frac{2\Delta_+\Delta_- + 2\varepsilon_a^2}{\Delta_+^2 + \Delta_-^2 + 2\varepsilon_a^2}\,\delta, \qquad (20)$$

where ε_a^2 is a small bias of order $O((\Delta x)^3)$, preventing clipping of smooth extrema.

The averaging-limiting procedure is valid for a single convection equation, implying that we should choose the quantities q to be the Riemann invariants of our equations. In the following we will consider averaging on (i) the components of the split flux-vectors $f^{\pm}$ as given by Eq. (17), (ii) variables related to the Riemann invariants, as used in [2] and (iii) the true Riemann invariants.

We start with (i). To justify the choice of the split flux-vectors we mention that the $f^{\pm}$ themselves are Riemann invariants associated with the matrices $E^{\pm} = \frac{\partial f^{\pm}}{\partial w}$, albeit only for $|u| < c$. It is tempting to write down the following second-order version of scheme (18):

$$\left[-\frac{\alpha}{\Delta x}E^+_{i-1}\right]\Delta_t w_{i-1} + \left[\frac{1}{\Delta t} - \alpha B_i + \frac{\alpha}{\Delta x}E^+_i - \frac{\alpha}{\Delta x}E^-_i\right]\Delta_t w_i$$

$$+ \left[\frac{\alpha}{\Delta x}E^-_{i+1}\right]\Delta_t w_{i+1} =$$

$$Bw_i - \frac{1}{\Delta x}\left\{(f_i^+ + \tfrac{1}{2}\overline{\Delta_i f^+}) - (f^+_{i-1} + \tfrac{1}{2}\overline{\Delta_{i-1} f^+})\right.$$

$$\left. + (f^-_{i+1} - \tfrac{1}{2}\overline{\Delta_{i+1} f^-}) - (f^-_i - \tfrac{1}{2}\overline{\Delta_i f^-})\right\}. \qquad (21)$$

The only change with respect to (18) is the explicit addition of the proper second-order terms on the right-hand side; the left-hand side is the same as in (18) in order to preserve the block-tridiagonal structure. The effect of the second-order terms is that f_i^+ is evaluated at the right boundary of cell i and f_i^- at the left.

The convergence history and solution for scheme (21) with N=64 are given in Figs. 4a and b. The solution is not as accurate as we expect from a second-order scheme, neither in the supersonic nor in the subsonic region (cf. Figs. 5b). There are two reasons for this. (a) In the supersonic regions the fluxes $f^{\pm}$ are not the Riemann invariants of the equations. (b) In a sonic point the matrices $E^{\pm}=\frac{\partial f^{\pm}}{\partial w}$ are continuous but not continuously differentiable, as required in a second-order method. The effect of this is clearly visible in the plot of u in Fig. 4b.

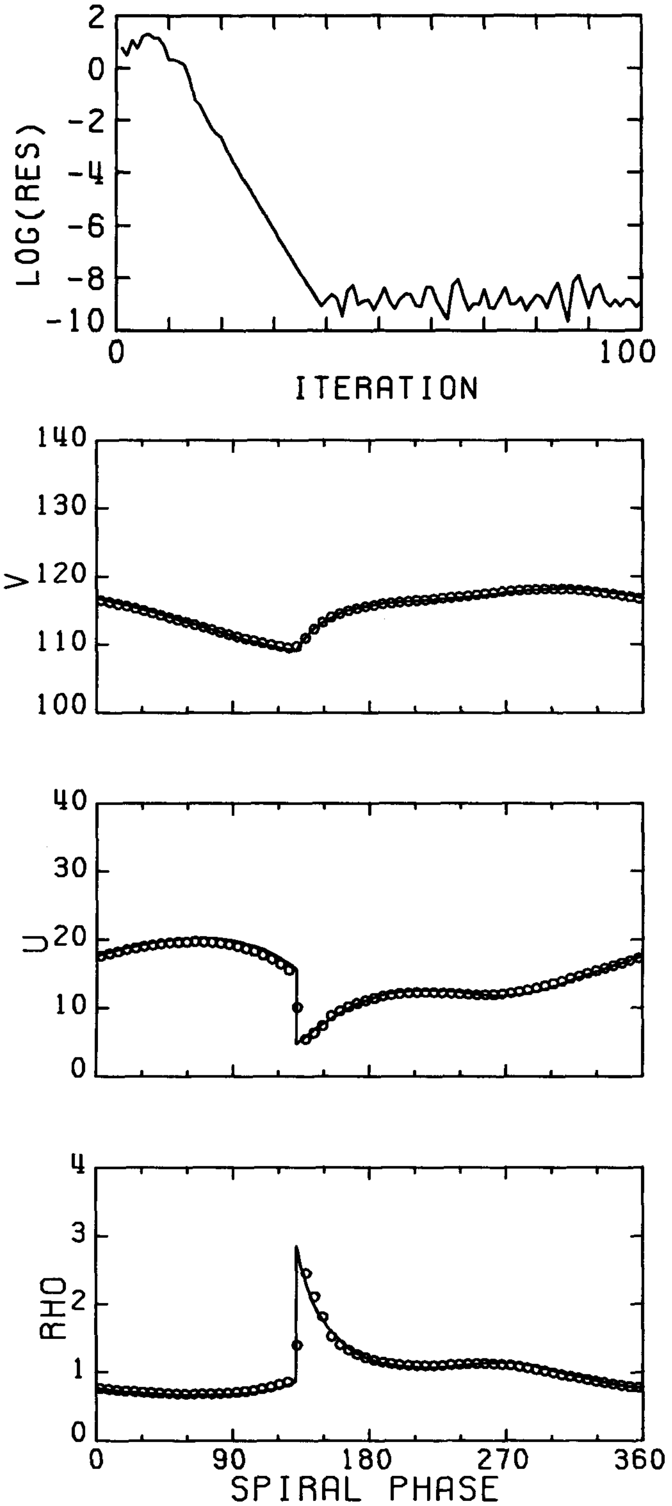

Fig. 4a. Convergence history and 4b second-order accurate solution for the flux-vector splitting scheme (21) with averaging procedure (20) based on the split fluxes (α = 1, ε = 0.5).

The bias vector ε_a^2 was given a fairly large value in the experiment of Fig. 4, implying weak limiting. For smaller values, or stronger limiting, the solution becomes non-unique, namely, different for different initial values. This, again, is an effect of the non-smoothness of $\partial f^{\pm}/\partial w$, worsened by the limiter. In brief, second differences of split fluxes, limited or not limited, should be avoided.

Continuing with (ii) we choose:

$$q = \begin{pmatrix} \ln\rho \\ u/c \\ v/c \end{pmatrix}, \quad \Delta_{i+\frac{1}{2}}q = \begin{pmatrix} \dfrac{\Delta_{i+\frac{1}{2}}\rho}{\frac{1}{2}(\rho_i+\rho_{i+1})} \\ \dfrac{\Delta_{i+\frac{1}{2}}u}{c} \\ \dfrac{\Delta_{i+\frac{1}{2}}v}{c} \end{pmatrix}, \quad \begin{pmatrix} \Delta_i\rho \\ \Delta_i u \\ \Delta_i v \end{pmatrix} = \begin{pmatrix} \rho\overline{\Delta_i q_1} \\ c\overline{\Delta_i q_2} \\ c\overline{\Delta_i q_3} \end{pmatrix} \quad (22)$$

We first evaluate ρ, u and v at both cell boundaries, then use these values to compute f_i^- at the left one and f_i^+ at the right one. It is necessary to evaluate the matrices $E_i^{\pm}$ on the basis of the same boundary values for proper convergence. Using mid-zone values of $E_i^{\pm}$, as in (21), the convergence process causes to end up in a limit cycle. The deviation from the steady state is largest on the subsonic side of the sonic point, suggesting that the limit cycle is caused by the non-smoothness of $E^{\pm}$ around the sonic point.

Convergence for the scheme with $E^{\pm}$ evaluated at the same position as $f^{\pm}$ was achieved within 90 steps for N=64 and ε_a^2=0.008, as in [2]. The resulting solution is almost indistinguishable from solution obtained with the explicit time-accurate scheme of [2]. Comparison with the first-order solution in Fig. 3 shows that the kink across the sonic point has disappeared, a result of the second-order approach.

We have also tried a different averaging procedure, somewhat closer to the switches in Eq. (66) of [5] than Eq. (20):

$$\bar{\Delta} = \frac{4\Delta_+\Delta_- + 2\varepsilon_a^2}{(|\Delta_+| + |\Delta_-|)^2 + 2\varepsilon_a^2}\,\delta \ . \quad (23)$$

This does not appear to significantly affect the convergence or the accuracy of the scheme.

Finally, we discuss the averaging (iii) applied to differences of the true Riemann invariants:

$$q = \begin{pmatrix} \frac{u}{c} - \ln\rho \\ \frac{u}{c} + \ln\rho \\ \frac{v}{c} \end{pmatrix}, \quad \Delta_{i+\frac{1}{2}}q = \begin{pmatrix} \dfrac{\Delta_{i+\frac{1}{2}}u}{c} - \dfrac{\Delta_{i+\frac{1}{2}}\rho}{\frac{1}{2}(\rho_i+\rho_{i+1})} \\ \dfrac{\Delta_{i+\frac{1}{2}}u}{c} + \dfrac{\Delta_{i+\frac{1}{2}}\rho}{\frac{1}{2}(\rho_i+\rho_{i+1})} \\ \dfrac{\Delta_{i+\frac{1}{2}}v}{c} \end{pmatrix},$$

$$\begin{pmatrix} \overline{\Delta_i \rho} \\ \overline{\Delta_i u} \\ \overline{\Delta_i v} \end{pmatrix} = \begin{pmatrix} \frac{\rho_i}{2}\,(\overline{\Delta_i q_2} - \overline{\Delta_i q_1}) \\ \frac{c}{2}\,(\overline{\Delta_i q_2} + \overline{\Delta_i q_1}) \\ c\,\overline{\Delta_i q_3} \end{pmatrix} . \qquad (24)$$

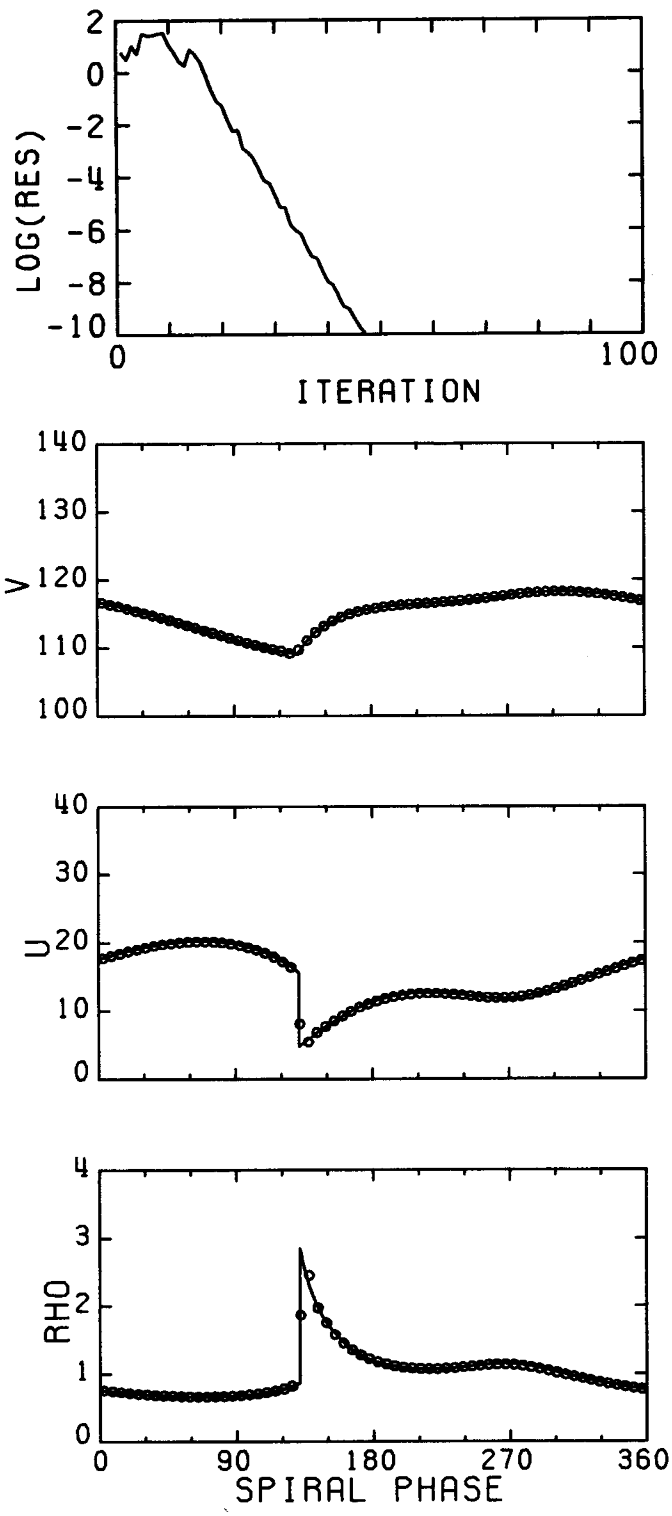

Fig. 5a. Convergence history and 5b solution with averaging procedure (20) based on the Riemann invariants (24) ($\alpha = 1$, $\varepsilon = 0.5$, $\varepsilon_a^2 = 0.008$).

We use $\varepsilon_a^2 = 0.008$ in the averaging procedure (20), as in [2], and evaluate $f_i^{\pm}$ and $E_i^{\pm}$ both from the same boundary values of ρ, u and v in zone i. Results are shown in Fig. 5. Convergence is significantly faster than for the previous second-order schemes. The solution is a notch better in the regions where the flow is smooth. Apparently , interpolating Riemann invariants yields the most efficient second-order scheme. This scheme is also more efficient than the first-order schemes of Figs. 2 and 3b, which require a mesh-refinement of about a factor 1/6 in order to match the accuracy of Fig. 5b (see [2], Table 1).

6. Conclusions

Our test of implicit upwind-differencing schemes for the Euler equations, including two different Riemann solvers lead to the following conclusions.

1. Quadratic convergence to a steady state incorporating a shock can be achieved with first-order upwind differencing.
2. Fast convergence requires a Riemann solver that allows continuous differentiation. Such a solver is provided by [4] (tested) or [10] (not tested).
3. Incomplete linearization in time of the implicit scheme may cause the iteration process to end up in a limit cycle. One economic way to avoid this is our β-scheme.
4. The second-order terms needed in second-order upwind schemes must not be computed directly as differences of split fluxes. Computation from differences of Riemann invariants performs best, especially in view of the necessary limiting process.
5. The decrease in convergence speed for a second-order upwind scheme is amply compensated by the increase in accuracy of the solution. The convergence speed is comparable to that of the non-conservative schemes of Napolitano and Dadone [13].

References

1. Beam, R.M., Warming, R.F., "An Implicit Finite-Difference Algorithm for Hyperbolic Systems in Conservation-Law Form", J. Comp. Phys. 22, 1976, pp. 87-110.
2. Van Albada, G.D., Van Leer, B., Roberts, W.W., "A Comparative Study of Computational Methods in Cosmic Gas Dynamics", Astron. Astrophys. 108, 1982, pp. 76-84.
3. Roe, P.L., "Approximate Riemann Solvers, Parameter Vectors, and Difference Schemes", J. Comp. Phys. 43, 1981, pp. 357-372.
4. Van Leer, B., "Flux-vector Splitting for the Euler Equations", in Proc. 8th International Conference on Numerical Methods in Fluid Dynamics, Aachen, June 1982, Lecture Notes in Physics 170, 1982, pp. 507-512, Springer, Berlin.
5. Van Leer, B., "Towards the Ultimate Conservative Difference Scheme. IV. A New Approach to Numerical Convection", J. Comp. Phys. 23, 1977, pp. 276-299.

6. Roberts, W.W., "Large-scale Shock Formation in Spiral Galaxies and its Implications on Star Formation", Astrophys. J. 158, 1969, pp. 123-143.
7. Harten, A., Lax, P.D., Van Leer, B., "On Upstream Differencing and Godunov-Type Schemes for Hyperbolic Conservation Laws", SIAM Review 25, 1983, pp. 35-61.
8. Roe, P.L., "The Use of the Riemann Problem in Finite Difference Schemes", in Proc. 7th International Conference on Numerical Methods in Fluid Dynamics, Stanford/NASA Ames, June 1980, Lecture Notes in Physics 141, 1980, pp. 354-359, Springer, Berlin.
9. Van Leer, B., "On the Relation between the Upwind-Differencing Schemes of Godunov, Engquist-Osher and Roe", SIAM J. Sci. Stat. Comput. 4, 1983, in press.
10. Osher, S., Chakravarthy, S., "Upwind Schemes and Boundary Conditions With Applications to Euler Equations in General Geometries", to appear in J. Comp. Phys., 1983.
11. Steger, J.L., Warming, R.F., "Flux Vector Splitting of the Inviscid Gasdynamic Equations With Application to Finite Difference Methods", J. Comp. Phys. 40, 1981, pp. 263-293.
12. Woodward, P.R., "On the Nonlinear Time Development of Gas Flow in Spiral Density Waves", Astrophys. J. 195, 1975, pp. 61-73.
13. Dadone, A., Napolitano, M., "An Implicit Lambda Scheme", AIAA paper nr. 82-0972, AIAA-ASME 3rd Joint Thermophysics, Fluids, Plasma and Heat Transfer Conference, St. Louis, Missouri, June 1982.

END